

UO₂ solubility measurements in Li and Na cryolite-based melts.

NADIR H., ALLIBERT M., BOEN R.*

Laboratoire de Thermodynamique et Physico Chimie Métallurgiques.

(associated with CNRS, INPG and UJF)

ENSEEG – BP75

38402 Saint Martin d'Hères – France.

*CEA – VALRHÔ – BP171 – 30205 Bagnol sur Cèze – France.

The solubility of UO₂ sintered pellets was measured by dipping the pellets into a fluoride bath and analyzing the U content of the melt as function of time. The melts used were Li₃AlF₆, Na₃AlF₆ and CaF-BaF₂ mixtures at temperatures ranging from 1000 to 1300°C. Several ratio of fluoride were studied as well as Al₂O₃, ZrO₂ or CaO containing cryolites. The solubility was found to be dependent on the presence of aluminum fluorate ions. It is low, about 0.04 wt%, with alkaline earth fluorides, higher with LiF, about 0.5 wt%, but it reaches up to 7 wt% with Li or Na cryolites. It is higher with Li than with Na. The presence of other oxides reduces the UO₂ solubility, likely because the oxygen dissolution capacity by formation of complex aluminum oxi-fluoride ions is limited. The UO₂ solubility was found to increase with temperature with cryolites but was almost temperature insensitive for CaF₂-BaF₂ melts. The dissolution enthalpy deduced from the temperature dependence of the solubility is 74 kJ/mol of UO₂ in Na₃AlF₆ and 86 kJ/mol in Li₃AlF₆.

I INTRODUCTION.

UO₂, when used as a nuclear fuel, is inserted in metallic tubing made of zircalloy or stainless steel. After its use in a power generator this assembly is dismantled to treat the spent fuel for actinides extraction and fission product elimination. For this the metallic tubes are sheared and the actinide oxides are dissolved into nitric acid. After this treatment the metallic pieces may be stored as a nuclear waste after pressing or melting. However these pieces are contaminated by uranium and any cleaning process would be beneficial for their storage.

A novel conditioning process (1) has been developed at the French nuclear agency center of Marcoule (CEA/DRDD/SCD) consisting in melting the metallic pieces in a cold crucible induction furnace. In this process a slag may be added to the load so that some of the remaining UO₂ could be dissolved and thus removed from the final ingot. By finding a convenient slag the residual actinide activity could be concentrated in a small amount of slag that may be treated apart.

The purpose of the present study was to find a effective solvent of uranium oxide and possibly zirconium oxide, as both may be present as mixtures in the waste because some mixing occurred during the irradiation period between the nuclear fuel and the zirconia passivation layer on the zircalloy.

In the novel process cited above zirconium and stainless steel are always melted together because they form low melting temperature alloys. The operating temperature ranges from 1000 to 1200°C depending on the alloy composition. It is difficult to find low melting point oxides that are not reduced by zirconium. But this temperature range corresponds to the melting points of cryolite-based salts that are well known (aluminum industry) to dissolve reasonable amounts of oxides.

It is the reason why UO₂ solubility measurements were undertaken in various fluoride-based melts.

II EXPERIMENTAL.

The experimental assembly is presented in Fig.1.

A 8mm diameter, 12mm long, sintered UO_2 cylinder is hold by a graphite tong and immersed in the solvent fluoride inside a 30mm diameter graphite crucible. An argon atmosphere is maintained to protect the graphite from burning in air. Only the graphite holder gets out of the induction heated graphite crucible, through the lid, and is connected to a motor with a speed regulator. This allows the stirring of the oxide salt interface to accelerate the diffusion of dissolved species. The rotation speeds ranged from 120 to 600 rpm.

Salt samples were taken by quenching the melts on cold steel rods and were analyzed for U by ICP after dissolution in perchloric acid. The kinetics was measured by taking six to eight 200mg to 400mg samples for each run that lasted 1 to 2 hours. It was characterized by a simple diffusion boundary layer model that leads to the following relationship:

$$\ln \frac{C^*}{C^* - C} = k \frac{A}{V} t \quad 1$$

where C is the instant concentration of UO_2 in the salt (wt%), C^* is the equilibrium concentration, k is a mass transfer coefficient (cm/sec), A is the interfacial area between the UO_2 cylinder and the melt (sq.cm), V is the melt volume (cubic cm) in which C is measured, and t is the time (seconds).

Only a thin layer of oxide was removed during each run with an erosion of about a few microns per second at the highest rate. The erosion rate is:

$$U = \frac{r_l}{r_s} k (C^* - C) \quad 2$$

where ρ_l and ρ_s are the specific masses respectively of the liquid salt and the solid oxide. The maximum rate U° is reached at the beginning of the dissolution into a UO_2 free salt ($C=0$). An example of the composition evolution during the dissolution experiment is given in Fig.2. The mass transfer determination on the same run is presented in Fig.3.

III RESULTS.

Stoichiometric lithium and sodium cryolites, as well as the 30% CaF_2 - 70% BaF_2 melts, were studied at various temperatures.

The results are presented in Table I.

Solubility.

The solubility variation with temperature may be represented by the enthalpy of the dissolution reaction: Pure solid $\text{UO}_2 \Rightarrow 1\text{wt}\% \text{UO}_2$ in solution at infinite dilution in the fluoride.

With these reference states and provided the infinite dilution assumption is valid, i.e. no variation of the UO_2 activity coefficient with the UO_2 content in the salt within the experimental composition range:

$$\Delta H_d - T \Delta S_d = -RT \ln(\% \text{UO}_2) \quad 3$$

The standard dissolution enthalpy of UO_2 at 1wt% was found to be: 76 ± 4 kJ/mol in Na_3AlF_6 , 80 ± 10 kJ/mol for Li_3AlF_6 , the corresponding plot is presented in Fig.4. The solubility in CaF_2 - BaF_2 melts was too low and not accurate enough to allow the determination of a dissolution enthalpy.

The solubility decreased when the cryolite compounds Na_3AlF_6 (Fig.5) and Li_3AlF_6 (Fig.6) were diluted by LiF , NaF , KF or CaF_2 . The results reported in Fig.5 and 6 show that the solubility is almost a linear function of cryolite molar concentration.

Dissolution kinetics.

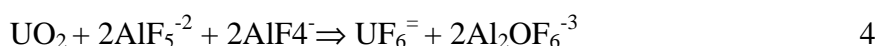
The kinetics of dissolution of UO_2 in the salts were characterized by a mass transfer coefficient k according to equation 1. This coefficient depends on stirring as shown in Fig.5. The representation of these values by a power function of the rotation velocity of the stirrer gives exponents above 0.6. In usual correlation such values are considered to characterize a mass transfer controlled by diffusion.

The mass transfer coefficients vary with temperature as shown in Fig. 6. The activation energy of the process, according to the Arrhenius plot shown in Fig.6 was found to be about 45kJ/mole for Na_3AlF_6 , 60 kJ/mole for Li_3AlF_6 and 180kJ/mol for $\text{CaF}_2\text{-BaF}_2$. Such a difference between cryolite medium and alkaline earth fluorides might be due to a change in the limiting factor if the measurements on $\text{CaF}_2\text{-BaF}_2$ were reliable.

There is no significant effect of composition on the mass transfer coefficient for cryolites. For the $\text{CaF}_2\text{-BaF}_2$ solvent it seems that Ba favors the dissolution kinetics, may be by favoring diffusion.

IV DISCUSSION

The well known fact that oxide solubility is higher in cryolites than in alkaline or alkaline hearth fluorides has been explained (2,3) by the formation of oxifluoro aluminates ions such as $\text{Al}_2\text{OF}_6^{-3}$, at low oxide concentration, and $\text{Al}_2\text{O}_2\text{F}_4^{-}$, at high oxide concentration. The speciation that has been proposed for cryolitic melts (4) involves alkaline cations and the following anions: F^- , AlF_6^{-3} , AlF_5^{-2} , AlF_4^{-} . The abundance of these anions changes with the nature of the alkaline cation has been estimated by Zhou (5). His results are presented in Table II and compared to the present measurements of UO_2 solubility at 1100°C. It seems that this solubility follows the same trend as the F^- anions, i.e. the basicity of the melt, and not the relative abundance of the fluoro-aluminates ions. This behavior could be explained by the formation of fluoro-uranate ions that is sensitive to basicity, for instance with the following simplified reaction:



The abundance of AlF_4^{-} and AlF_5^{-2} ions change continuously, but in opposite directions, from a Li medium to a K medium. To explain the observed behavior of solubility one have to assume that the stability of UF_6^{-} ion also varies with the nature of the cation. The equilibrium constant of reaction 4, using anion activities given by Zhou and the molar fractions of UF_6^{-} and $\text{Al}_2\text{OF}_6^{-3}$ at saturation by UO_2 , is lower for Li cryolite than for sodium cryolite,. This could mean that fluoro-uranates ions are less stable in Li cryolite than in Na cryolite, despite the higher solubility value found for UO_2 .

Due to the complex speciation in the cryolite melts it is difficult to give a convincing interpretation of these few results. Nevertheless the sensitivity of UO_2 solubility to the presence of other oxides (Al_2O_3 or ZrO_2) pleads for the presence of oxygen in oxi-fluoro-aluminates ions. From that point of view UO_2 is not different from any other oxide. This dependence could have lead to an underestimation of the solubility because of some oxygen remaining in the melt. No large amount were detected by X-Ray diffraction or Raman spectroscopy on solid salts but these techniques are not very sensitive and amounts of the order of 0.1 mole % are possible. The observed change in UO_2 solubility is of the order of 0.1 mole % per mole % of alumina. The UO_2 solubility is not determined with a reproducibility

better than 0.1%, so the present results are not significantly affected by oxygen contents in the melt lower than about 1 mole %.

With respect to the objective of processing oxide-containing metallic wastes the addition of AlF_3 to the cryolites would have been favorable to UO_2 or ZrO_2 dissolution but the processing temperature is such that some volatilization might occur. This last point has not been checked over.

CONCLUSION

A simple experimental device was used to measure the UO_2 solubility in cryolitic melts, with or without other oxides, to evaluate the possibility offered by these melts to remove radioactive oxides associated with nuclear fuel claddings. The dissolution kinetics was also measured for a cylinder of sintered UO_2 rotating in the salt.

Unexpectedly a good solubility was found in Li cryolite that is interesting for the process because LiF is more stable than NaF or KF in presence of a reducing element such as Zr (formation and volatilization of ZrF_4). Solubility data at 1100°C and 1200°C are given for stoichiometric Li, Na and K cryolites.

The erosion rate of an UO_2 layer in agitated cryolitic melt was found to be of the order of 1 m/s in Li_3AlF_6 or Na_3AlF_6 . A short residence time of the oxide contaminated metallic hulls in a fluoride melt above the metallic liquid pool during the processing may be sufficient to remove a significant part of the UO_2 contamination.

REFERENCES

- 1- BERTHIER P., BOEN R., PICCINATO R., LADIRAT C., "Reducing the radiotoxicity of PWR cladding hulls by cold crucible melting" Proceedings of RECOD 94, London, April 1994.
- 2- DEWING E., THONSTAD J., Met. Trans.B, vol 28B, 1997, pp1089-1093.
- 3- ROBERT E., OLSEN J.E, DANEK V., TIXHON E., ØSTVOLD T., GILBERT B., J.Phys.Chem B,1997, 101, pp 9447-9457.
- 4- GILBERT B., ROBERT E., TIXHON E., OLSEN J.E., ØSTVOLD T., Inorg.Chem., 1996, 35, pp 4198-4210.
- 5- ZHOU H. Thesis: "Thermodynamic studies of Cryolite Based Melts"
Institute for Inorganic Chemistry, NIT, University of Trondheim, Norway, 1991

Table 1: Measured values of UO_2 solubility and mass transfer coefficient k for the oxide dissolution. U° is the maximum erosion rate reached when the salt is oxide-free.

Salt	Composition. (wt%)	T (°C)	UO_2 solubility (wt%)	Rotation (rpm)	k ($\mu\text{m/s}$)	U° ($\mu\text{m/min}$)
Na_3AlF_6	100	1050	3.0	250	56	20
Na_3AlF_6		1100	4.1	250	69	34
Na_3AlF_6		1150	5.0	250	73	43
Na_3AlF_6		1200	6.0	250	85	60
Na_3AlF_6		1100	4.0	120	46	20
Na_3AlF_6		1100	4.0	180	62	30
Na_3AlF_6		1100	4.0	250	70	33
Na_3AlF_6		1100	3.9	300	82	40
Na_3AlF_6		1100	4.1	400	93	45
Na_3AlF_6		1100	4.1	500	113	55
Na_3AlF_6		1100	4.1	600	100	50
$\text{Na}_3\text{AlF}_6\text{-KF}$	80-20	1100	3.5	250	96	40
$\text{Na}_3\text{AlF}_6\text{-NaF}$	86.4-13.6	1100	3.2	250	66	25
$\text{Na}_3\text{AlF}_6\text{-NaF}$	62-38	1100	3.2	250	62	24
$\text{Na}_3\text{AlF}_6\text{-LiF}$	80-20	1100	2.6			
$\text{Na}_3\text{AlF}_6\text{-Al}_2\text{O}_3$	95-5	1100	1.0	250	50	6
$\text{Na}_3\text{AlF}_6\text{-Al}_2\text{O}_3$	98-2	1100	1.8	250	50	11
$\text{Na}_3\text{AlF}_6\text{-Al}_2\text{O}_3$	Al_2O_3 sat	1100	0.2			
$\text{Na}_3\text{AlF}_6\text{-ZrO}_2$	96-4	1100	2.0	250	35	8
$\text{Na}_3\text{AlF}_6\text{-ZrO}_2$	98-2	1100	2.5	250	60	18
$\text{Na}_3\text{AlF}_6\text{-ZrO}_2$	ZrO_2 sat	1100	0.9			
$\text{Na}_3\text{AlF}_6\text{-CaO}$	96-4	1100	1.5	250	70	12
$\text{Na}_3\text{AlF}_6\text{-CaF}_2$	65-35	1200	2.9	250	70	24
$\text{Na}_3\text{AlF}_6\text{-CaF}_2$	82.5-17.5	1200	3.6	250	81	35
Li_3AlF_6	100	1000	2.6	250	68	20
Li_3AlF_6	100	1100	5.6	250	95	60
Li_3AlF_6	100	1200	7.2	130	90	70
Li_3AlF_6	100	1200	7.3	250	140	110
Li_3AlF_6	100	1200	7.3	350	188	152
$\text{Li}_3\text{AlF}_6\text{-CaF}_2$	60-40	1200	4.1	250	85	40
$\text{Li}_3\text{AlF}_6\text{-CaF}_2$	80-20	1200	5.2	250	95	55
$\text{Li}_3\text{AlF}_6\text{-LiF}$	75-25	1000	1.4			
$\text{Li}_3\text{AlF}_6\text{-LiF}$	50-50	1000	1.0			
$\text{Li}_3\text{AlF}_6\text{-LiF}$	0-100	1000	0.5			
$\text{Li}_3\text{AlF}_6\text{-ZrO}_2$	ZrO_2 sat	1200	3.0			
$\text{CaF}_2\text{-BaF}_2$	30-70	1200	0.04	250	40	0.25
$\text{CaF}_2\text{-BaF}_2$	30-70	1250	0.027	150	43	0.2
$\text{CaF}_2\text{-BaF}_2$	30-70	1250	0.033	250	65	0.4
$\text{CaF}_2\text{-BaF}_2$	30-70	1250	0.029	350	94	0.5
$\text{CaF}_2\text{-BaF}_2$	30-70	1300	0.04	250	84	0.6
$\text{CaF}_2\text{-BaF}_2$	10-90	1250	0.03	250	83	0.4
$\text{CaF}_2\text{-BaF}_2$	50-50	1250	0.04	250	57	0.55

Table II: Measured UO_2 solubility at 1100°C compared to anions activities estimated by Zhou (5). The equilibrium constant of reaction 4 is evaluated from these activities and molar fraction of UO_2 in solution.

M in M_3AlF_6	Li	Na	K
F^- activity	0.48	0.36	0.50
AlF_4^- activity	0.22	0.10	0.09
AlF_5^{2-} activity	0.02	0.16	0.35
AlF_6^{3-} activity	0.28	0.38	0.06
UO_2 solubility mole%	3.36	3.2	5.7
UO_2 solubility wt%	5.6	4.1	6
K equilibrium 4	0.51	7.81	5.36

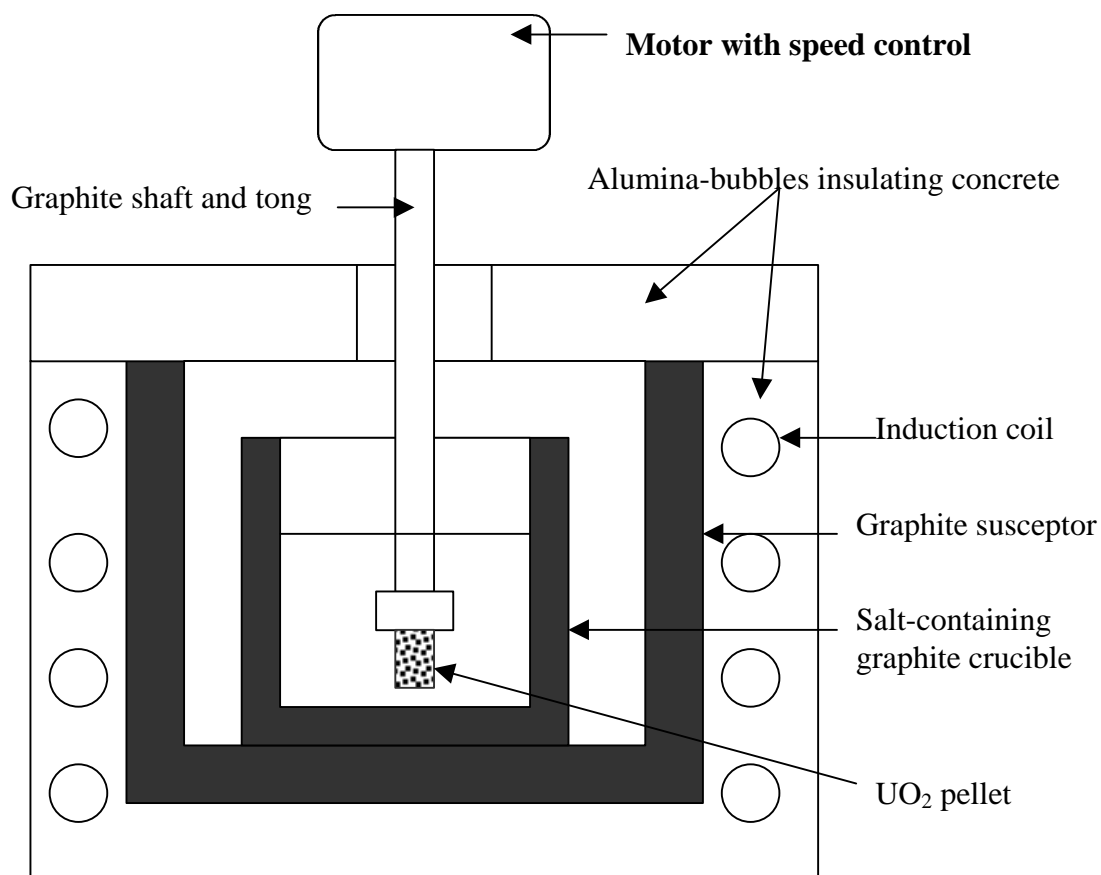


Fig. 1: Schematic representation of the experimental assembly used for UO_2 dissolution measurements.

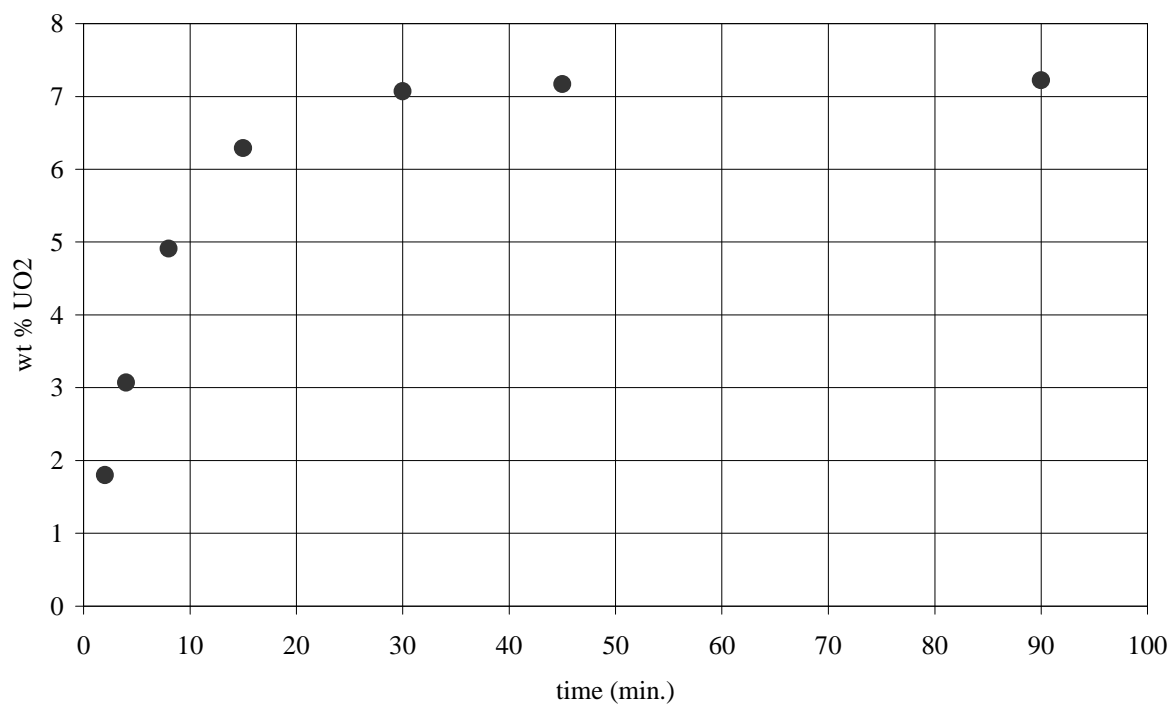


Fig 2: Example of concentration evolution with time with UO_2 dissolution in Li_3AlF_6 at 1200°C and 350rpm. Equilibrium is almost reached at 30 min.

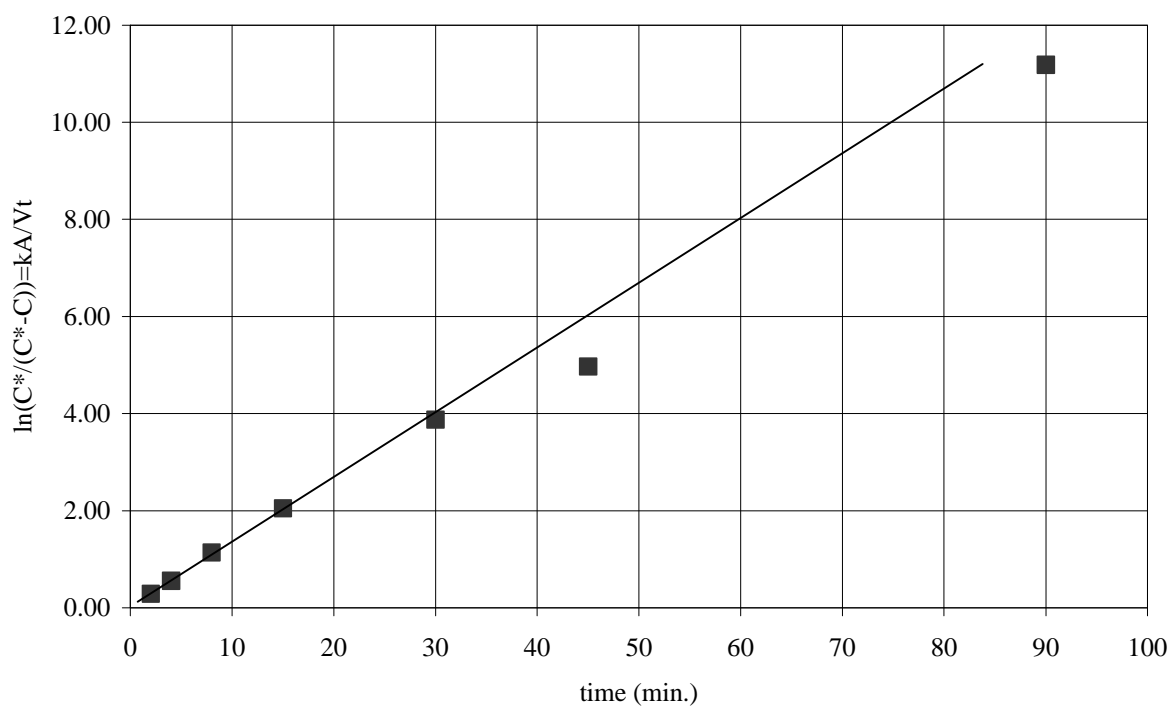


Fig 3: Example of determination of mass transfer coefficient for Li_3AlF_6 dissolution at 1200°C and 350rpm. Only the results for time below 30 min. are taken into consideration because for longer times the system is too close to equilibrium to be sensitive to kinetics.

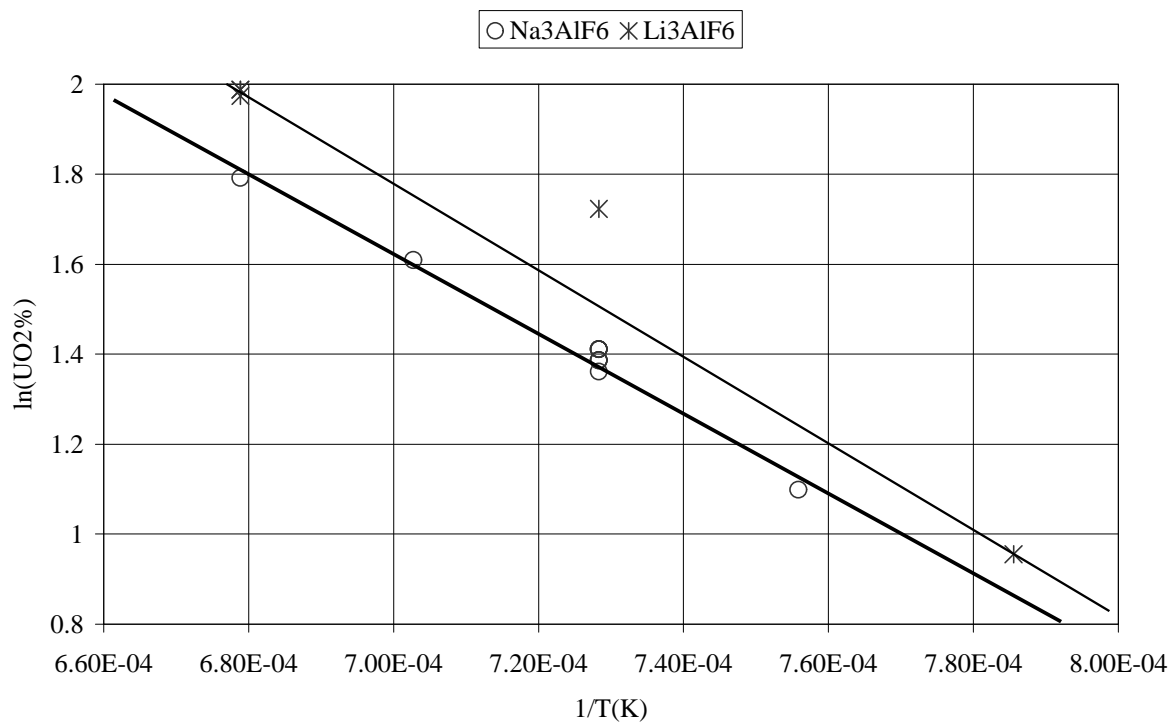


Fig. 4 : Dependence on temperature (Kelvin) of the measured UO_2 solubility (wt %) in Li and Na cryolites.

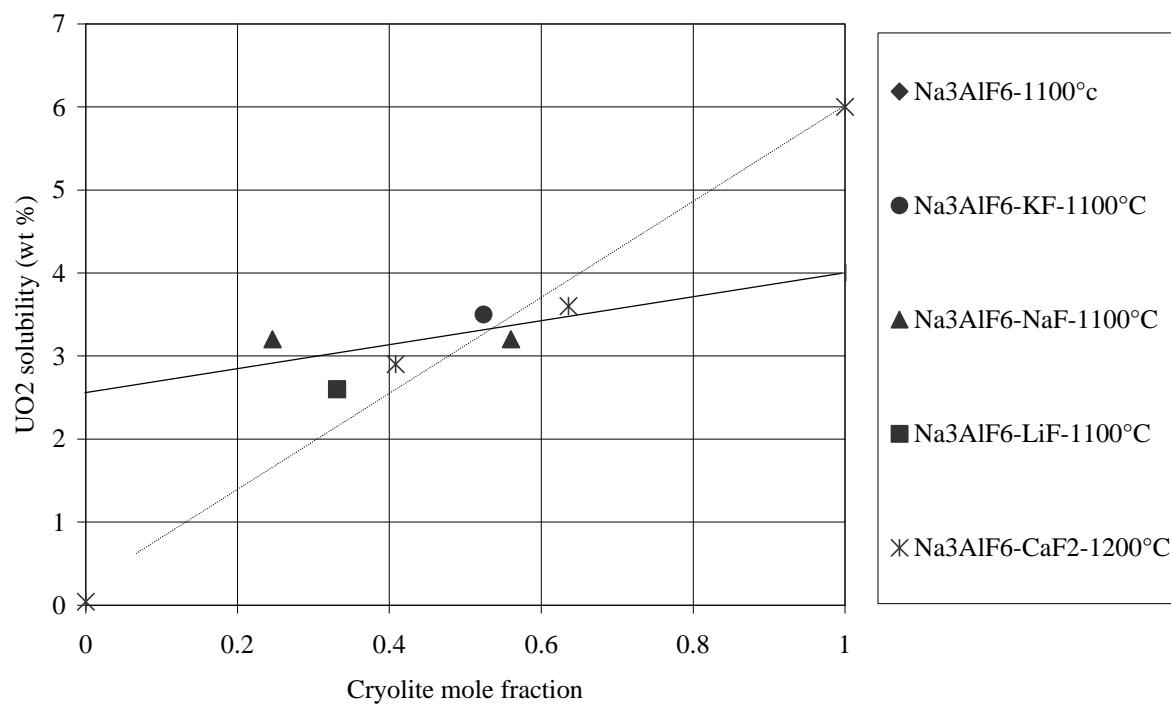


Fig. 5 : Change of UO_2 solubility with Na_3AlF_6 dilution.

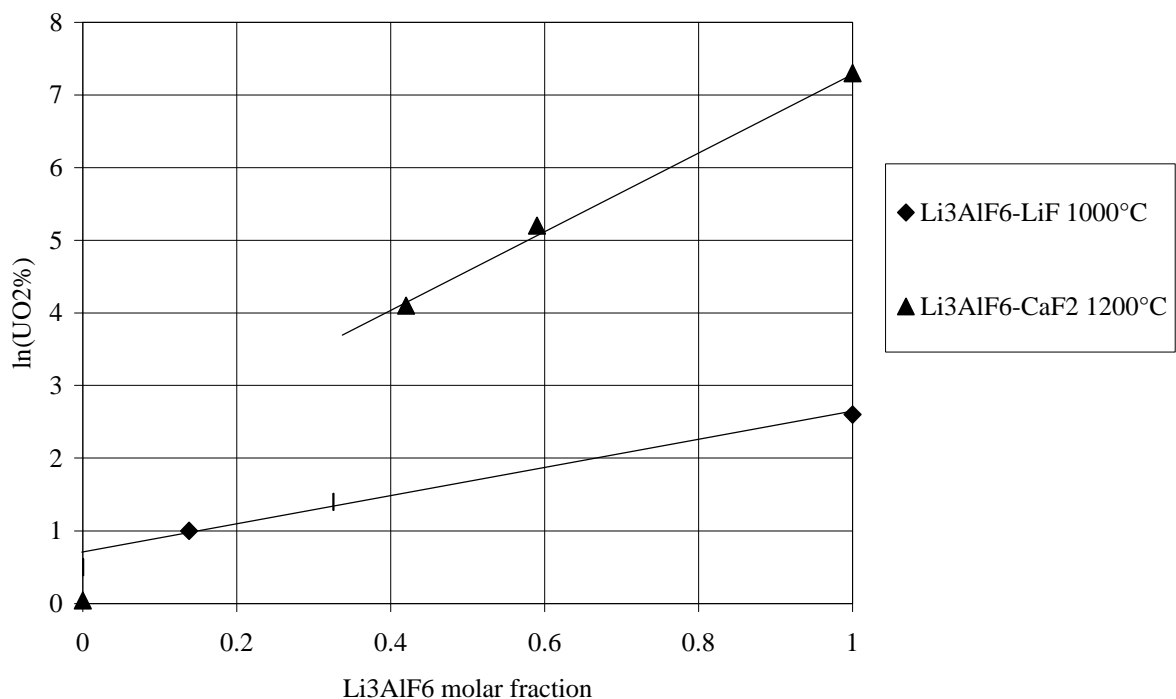


Fig 6 : UO_2 solubility evolution with Li_3AlF_6 dilution.

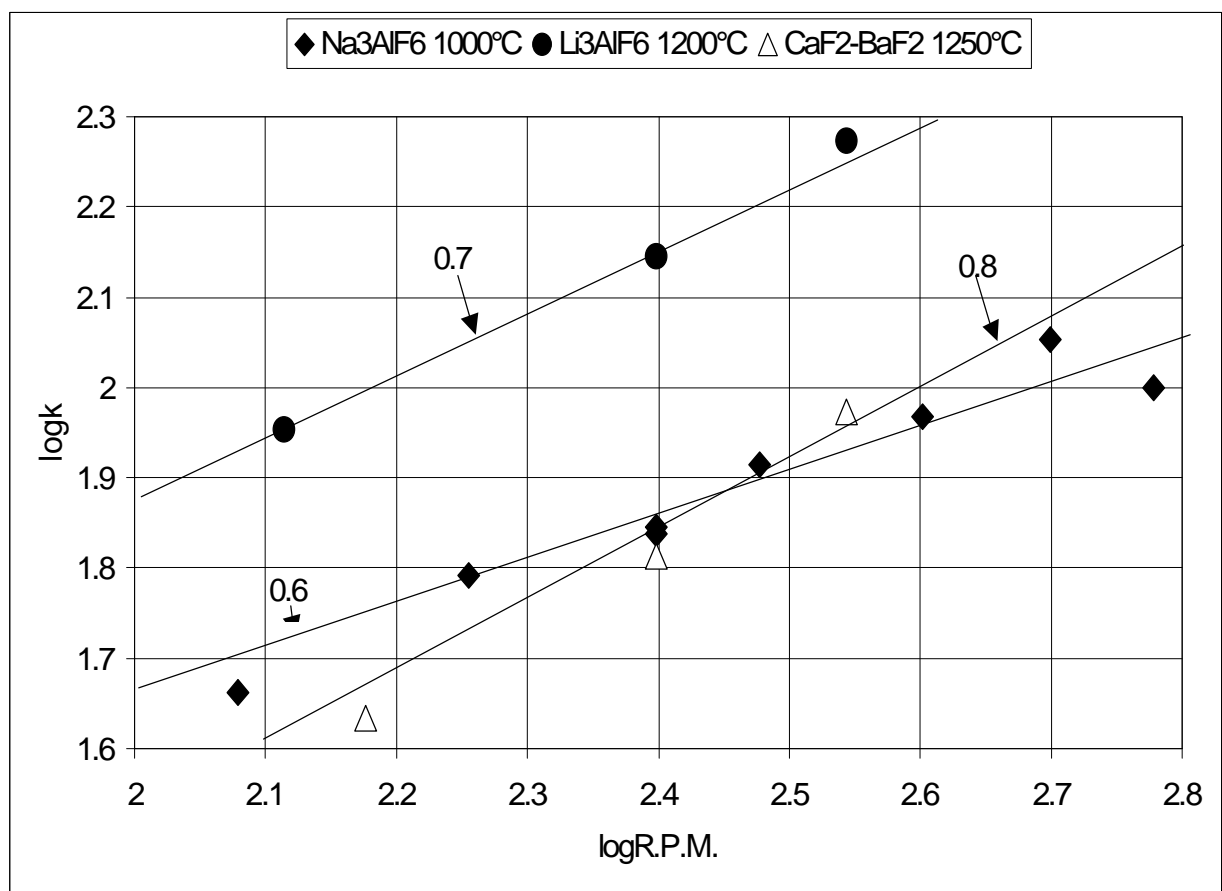


Fig 7 : Dependence of the mass transfer coefficient on stirring.

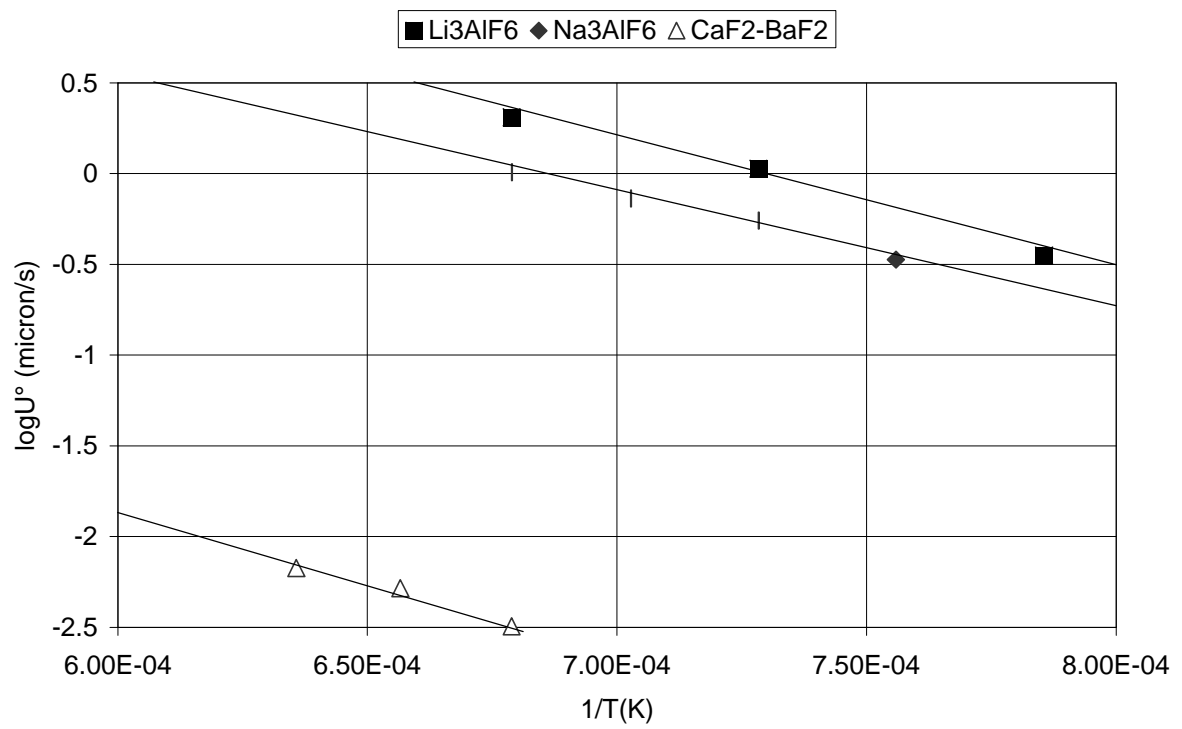


Fig 8 : Temperature dependence of the maximum erosion rate U° (in absence of dissolved UO_2) for three salts.